

Redesign and taking into service of a new test facility for nozzle flow experiments

Bron O. *
Tel: +46 8 790 7434
bron@egi.kth.se

Freudenreich K. **
Tel: +46 8 790 7480
kai@egi.kth.se

Fransson T. H. ***
Tel: +46 8 790 7475
fransson@egi.kth.se

Royal Institute of Technology
Chair of Heat and Power Technology
10044 Stockholm, Sweden
Fax: + 46 8 204161

ABSTRACT

A prerequisite for aeroelastic stability investigations in turbomachines is the understanding of the unsteady aerodynamic forces acting on the blades. Considering the lack of experimental data, fundamental studies are needed to obtain precise insight into aeroelastic phenomena associated with oscillating shock waves. The aim, in the present study, is to further understand the behaviour of travelling pressure waves in non-uniform transonic flows at different operating conditions. A project has been started to investigate the unsteady interaction of upstream propagating pressure waves with a shock in transonic convergent-divergent nozzles at different inlet boundary layer conditions. The emphasis is on how this interaction can affect the unsteady pressure distribution on the surface and lead to unstable configurations. This paper intends to present the facility in which those experiments are being performed, and give an overview of the intended future modifications and investigations. Different test objects and their instrumentation will be presented as well as the first preliminary results.

NOMENCLATURE

M	[-]	Mach number
Re	[-]	Reynolds number
U	[m.s ⁻¹]	Inlet Velocity in Free Stream
p	[kPa]	Total pressure
v	[m ² .s ⁻¹]	Fluid viscosity
D	[m]	Characteristic BL Length

Subscripts

1,2	Inlet, Outlet
s	Static
t	Total/Stagnation value
∞	Free Stream

Abbreviations

2D	Two Dimensional
3D	Three Dimensional
ADC	Analog Digital Converter
BL	Boundary Layer
L2F	Laser-Two-Focus Anemometry
LDA	Laser-Doppler-Anemometry
PIV	Particle Image Velocimetry
PSU	Pressure Standard Units
SBLI	Shock Boundary Layer Interaction

* Ph.D. Student: Ecole Centrale de Lyon, France
Chair of Heat and Power Technology, Sweden

** Ph.D. Student Chair of Heat and Power Technology

*** Prof. Chair of Heat and Power Technology

BACKGROUND

Transonic flows about streamlined bodies are strongly affected, particularly near the shock location, by unsteady excitations. Experimental and computational studies [1,3] have shown that the unsteady pressure distribution along the surface of an airfoil or a cascade blade in unsteady transonic flow exhibits a significant bulge near the shock location. Tijdeman and Seebass [11] reported that the unsteady pressure bulge and its phase variation resulted from non-linear interaction between the mean and unsteady flow. This non-linear interaction causes a shift in the shock location, which produces the observed large bulge in the unsteady pressure distribution.

Studies [5] on choked flutter around a single airfoil have shown that, in unsteady transonic flows, the shock motion can be critical regarding to the self-exciting oscillation of the airfoil. It was also found that the mean flow gradients are of high importance regarding the time response of the unsteady pressure distribution on the airfoil surface. Moreover, numerical computations [4] have shown that the exact location of the transition point could strongly affect the prediction of stall flutter.

Further studies [2] suggested that this sharp rise in the unsteady pressure distribution was due to the near sonic condition, and that the near-sonic velocity acts as a barrier they called *acoustic blockage* preventing acoustic disturbances from propagating upstream in a similar way to the shock in transonic flows. A transonic convergent-divergent nozzle experimentally investigated by Ott et al. [10] was thereafter used as a model to investigate the non-linear acoustic blockage. Analytical and numerical computations [6,7,8,9] were then carried out to analyse and quantify the upstream and downstream propagation of acoustic disturbances in the nozzle.

OBJECTIVES

Considering the lack of experimental data to analyse and better understand basic phenomena that occur in turbomachines, a project was started at the Chair of Heat and Power Technology, Sweden. The aim is to further investigate basic unsteady internal transonic flow interactions. The objective, in the long run, is to get precise insight into aeroelastic phenomena and determine which parameter influence aeroelastic boundaries, and in which way.

The first task in this project was therefore to build a facility that would allow an easy and flexible change of test objects, as well as different inlet conditions to be investigated. The facility should also allow multiple measuring techniques and thus feature a good optical access for LDA, L2F, or Schlieren visualisations, as well as an easy access for surface pressure taps.

The following paper intends to present such facility as well as the different test objects and instrumentation, and its future modifications in the future tasks of this project.

THE NEWLY DESIGNED FACILITY

The overall wind tunnel facility

The Chair of Heat and Power Technology is equipped with a 1MW compressor which can deliver a mass flow up to 4.7 kg/s at 4 bars and 30°C. A cooling system also allows a temperature adjustment from 180°C down to 30°C with an accuracy of ± 0.1 degree. The flow can thereafter be redirected either into a test turbine or a conventional wind tunnel facility, as sketched in Fig. 1.

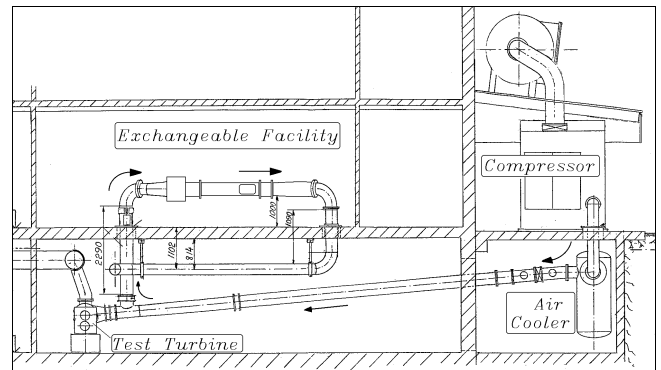


Figure 1: Overall Facility at HPT

The particularity, in the latter case, is that the test section including the settling chamber is exchangeable and allow different facilities to be inserted and investigated using the same air supply.

A set of valves thereafter allows the control of the mass flow and the pressure level within the test section (Fig.2). An exhaust gas fan is placed downstream of the outlet valve in order to suck the air out to the atmosphere.

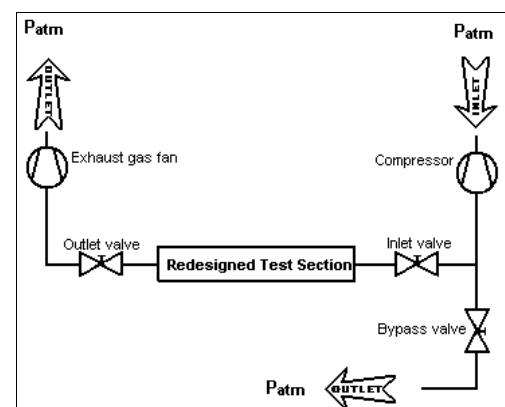


Figure 2: Sketch of the air supply

The supersonic test section

At an early status of the project the Chair of Heat and Power Technology received a supersonic wind tunnel test section fitting into the test section location. The rather small settling chamber of 250 mm x 250 mm is equipped with a flow straightened and turbulence grids. A first contraction in the horizontal plane guides the air flow into a 250 mm high, 100 mm wide inlet into a flexible de Laval nozzle on the upper and lower wall.

The height of the throat can be adjusted using a piston to accelerate the flow from low subsonic up to $M_1=2.75$ in the 100 mm x 106 mm test object section. The flat side walls are equipped with 388x163 mm optical glass windows at the test object section. They provide excellent conditions for optical measurement techniques as Schlieren technique, Particle Image Velocimetry (PIV), Laser-Two-Focus Anemometry (L2F) and Laser-Doppler-Anemometry (LDA). Figure 3 shows the old test section with the demounted front side wall. The flexible metal sheets on the upper and lower wall extend far into the test object section. They are not parallel and open in a sharp step to the channel exit height of 120 mm.

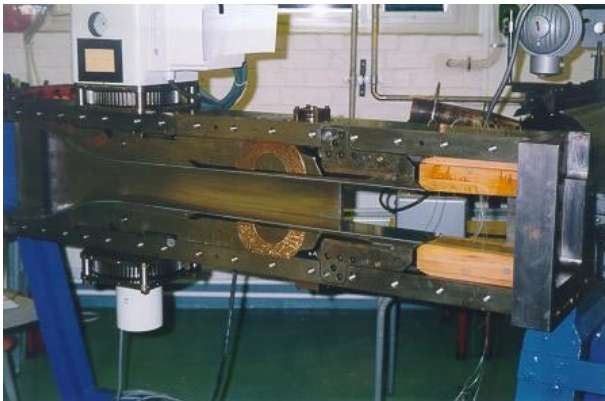


Figure 3: Old test section with a de Laval nozzle

Since the disturbing end of these sheets could not be changed, a completely new inlet contraction and test object section was designed to replace the flexible de Laval nozzle. As the already existing settling chamber and first horizontal contraction were located upstream and decoupled from the flexible de Laval nozzle, both were kept in the design of the new test facility. In order to fulfil the requirements of the test objects and the geometric boundary conditions the following design specifications were formulated:

1. Up- and downstream dimension fit to inlet and outlet of the existing de Laval test section
2. Upper and lower wall curvature are identical
3. Existing side walls with the windows can be used, i.e. test object location remains where it is
4. The boundary layer can grow over a distance of about 250 mm between maximum contraction and test object
5. Homogeneous, parallel and steady flow into the test object section for $p_{t1} = 170$ kPa and $M_1 = 0.6$, no boundary layer separation
6. Optional boundary layer cut off on the lower wall in front of the test objects and controlled blow out to the atmosphere
7. Possible insert of different test objects on both upper and lower walls
8. Easy change of configuration through the side windows
9. Easy and large external access to the test object for pressure tubes and wires

10. Good optical accesses through upper test section wall for optical measurements or flow visualisations

The New Inlet Contraction

The design specifications 1 to 5 deal with the design of a new inlet contraction. Specifications 1 to 3 were translated into: The original channel width (100 mm), inlet height (250 mm) and outlet height (120 mm) were kept. The new channel height over the entire empty test object section was increased to 120 mm. Specifications 4 and partly 5: Slightly diffusing upper and lower walls between maximum contraction and test object compensated the growth of the boundary layer displacement thickness. The resulting opening angle had to be connected smoothly to the contraction curvature. The boundary layer displacement thickness was calculated with a boundary layer code to about 1.8 mm, the boundary layer thickness to about 14.5 mm at the inlet to the test object section [12].

To obtain the contraction curvature, fulfilling specification 5, two different approaches were followed:

The first one was extremely simple: For the contraction curvature a 5th-order polynomial was assumed. This required six geometric boundary conditions, which were: Axial position and channel height at inlet (1st) and at maximum contraction (2nd). No discontinuity in the first and second derivative at the inlet (3rd + 4th), while the first and second derivative at the maximum contraction were given by the opening angle of the diffusing walls (5th + 6th). After solving the set of equations the criterion of no separation in the contraction and diffusing section was checked with the boundary layer code.

The second approach was more "classical": Morel [13] described a guideline for the design of two-dimensional wind tunnel contractions. Using inviscid flow analysis design charts were developed for a one-parameter family of wall shapes, based on two cubic arcs. The parameters were the maximum wall pressure coefficients at the inlet (as an indicator of the danger of separation at the inlet) and at the exit (related to the exit velocity non-uniformity and separation). Simple working forms of the separation criteria by Stratford [14] were used.

Both approaches resulted in very similar contraction curvatures and the geometry of the second approach was chosen.

The Modular Test Section

The specifications 6-9 required a highly flexible design for the section where the test objects and the optional boundary layer cut off are located.

In order to insert different test objects through the side windows on both upper and lower walls, and to have an easy access for instrumentation, the solution of mounting geometrically minimised test objects onto a model support part was chosen. Any test object which has a rectangular base will therefore fit in a support

piece. The dimensions were chosen to be 290mm long, 100mm wide and 25 mm thick to be able to exchange the test objects easily through the side window. The base part also features a large opening to the atmosphere so as to easily access and instrument the test objects from the outside (Fig 4). As a result, an excellent optical access from above can be obtained, for PIV or oil surface visualisations for instance, by inserting a small Plexiglas window into the upper support part (Fig 4). It should also be noted that the model support parts, placed on both upper and lower walls, were aligned to mirror each others and make the channel symmetrical. Of course, all connections between surfaces were carefully sealed with O-rings to prevent any leakage flow to the atmosphere. Moreover, all wind tunnel surfaces and connections between the different parts were manufactured with a very smooth finish to avoid boundary layer (BL) tripping.

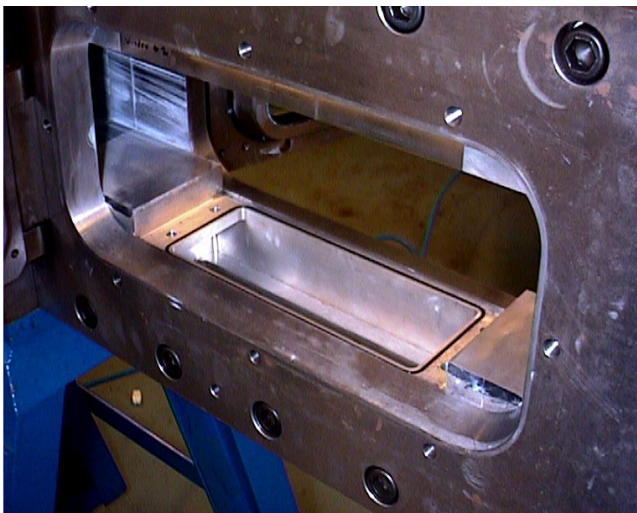


Figure 4: Base support part for test objects

In order to cut off the boundary layer to the atmosphere (requirement 6), the lower frame of the wind tunnel was designed with an opening just upstream of the test section location (Fig 7). The design was made in such way that the model support part on the lower wall is isolated from the other parts. The idea was to be able to lift it up together with the test object by simply inserting a flat plate under the whole support part. A special cut out enables the support part to be equipped with a “nose” part, which will thereafter “cut” the incoming flow and redirect the boundary layer to the atmosphere. Two different noses are available at the moment: a sharp one and a round one equipped with pressure taps on the leading edge. Two different situations can thereafter be encountered: either the pressure in the channel is above, or under atmospheric conditions. In the first case, the part of the incoming flow that is cut off by the nose will naturally go out to the atmosphere, whereas a vacuum pump is needed in the second case. The sensitive part is thereafter to control the outgoing mass flow accurately enough to properly cut off the incoming streamlines. Indeed, only streamlines located below the nose shall be cut off, whereas the

others, above the nose, shall remain parallel. A too high or too low mass flow would result in bend streamlines in the free stream over the nose part, that is to say a pressure gradient in the free stream as shown on Fig 5. The control of the outgoing mass flow will therefore be ensured by an accurate throttle valve manually adjusted.

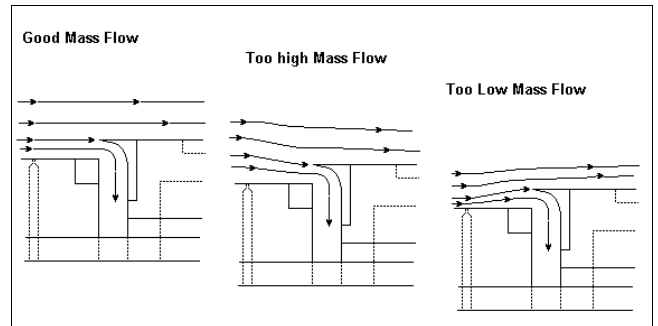


Figure 5: Effect of bad outgoing mass flow

Moreover, the adjustment of the valve has to be monitored easily. A first possibility is here to use the round nose equipped with pressure taps. Indeed, a maximum value for the total pressure shall be reached when the flow is inlined with the nose. The pressure in the settling chamber should be taken as a reference value to be reached. Nevertheless, any disturbances at the edge of the boundary point might induce a fluctuation of the leading point on the round nose. Hence, a sharp nose was foreseen less sensitive (Fig 6). In order to monitor the outgoing mass flow in this particular case, a second possibility is to insert aerodynamic probes from the upper wall and directly measure the pressure gradient at the inlet of the test section. However, as the boundary layer cut off has not been tested, it is not clear yet the influence of having a round or a sharp nose.

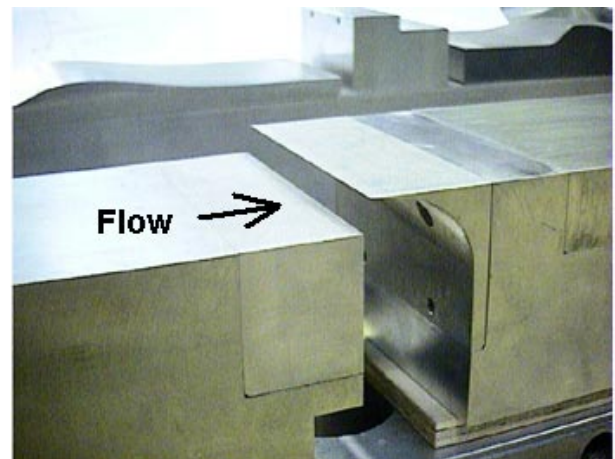


Figure 6: Boundary layer cut off with sharp nose

Finally, assuming that the nose is placed exactly at the edge of the boundary layer, the latter will be entirely blown out to the atmosphere. A new boundary layer will therefore grow from the leading edge of the nose, providing interesting test cases and useful information for transition or Shock Boundary Layer interaction (SBLI) studies.

On the other hand, a plug can also be inserted instead of a nose and thus provide a flat channel without boundary layer cut off. Three alternative configurations are therefore possible in the new test facility: a flat sharp, or a round nose, as sketched on Fig 7.

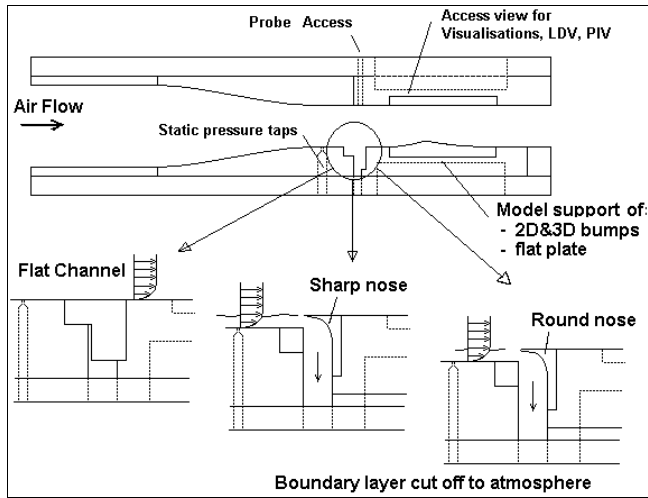


Figure 7: Three alternative configurations

To conclude, Mach and Reynolds numbers in the test section can be controlled independently. This provides a large range of possible Re values as summarised in the following table:

New test facility data:	
Mass flow	4.7 kg/s (4 bar, 297 K)
Total temperature	$297K \leq T_t \leq 453K$
Test section height	120 mm
Test section width	100 mm
Inlet Mach number	$0.02 \leq M \leq 0.8$
Charact BL. length	1.5 m or 0.065 m
Inlet Reynolds number	$43 \cdot 10^3 \leq Re \leq 27 \cdot 10^6$

TEST OBJECTS AND INSTRUMENTATION

Several test objects were designed to investigate 2D and 3D flow structure, and two geometries with bumps were chosen, a 2D and a 3D bump. Several test objects of each geometry were therefore manufactured to be equipped with different instrumentation.

steady state and unsteady pressure measurements, hot film measurements, Schlieren and oil surface visualisations can be performed on 2D and 3D transonic flows in this facility.

2D Sliding Bump

A first test object consists of a long 2D bump inserted in the lower base support part, which can slide through the width of the test section (Fig 8). This bump is equipped, on one side, with a row of 80 hot film sensors, and three staggered rows of 50 pressure taps each on the other side. As a results, both hot film and pressure measurements will be possible shortly

after each others by sliding the 2D bump to the same measurement location. The specific design of the pressure holes allows both steady and unsteady transducers to be inserted in any of the 150 pressure taps covering the main surface of the 290 mm long test object.

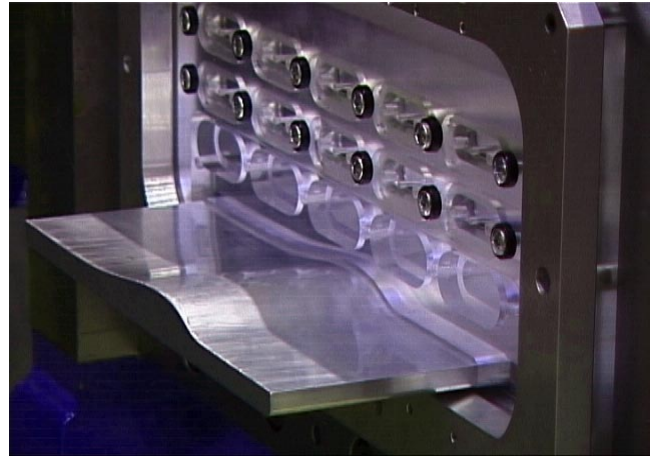


Figure 8: 2D Sliding Bump

The distance between two pressure taps located on the same row is 4.5 mm, and the staggered step between the different rows is 1.5 mm. As a result, sliding the 2D bump to successively position all three rows of pressure taps to the same location in the channel will finally provide a spatial resolution for pressure measurements of 1.5 mm. The single row of hot film sensors will also be positioned exactly at the same location to complete the measurement serie and provide information on the state of the BL. This procedure will then be repeated for several location across the channel width. A complete mapping of the steady and unsteady pressure and heat coefficient distribution along the 2D bump will thereafter be performed with the aim to characterise the side walls and corners effects.

Moreover, in order to slide the long 2D bump through the opening in the side walls, new Plexiglas windows had to be manufactured. With the aim to account for future configurations such as BL cut off (lifted support part and test object), the Plexiglas side windows were themselves foreseen with an exchangeable part, so called "small cassette", in which a special cut out with the 2D bump shape, should be located. The idea was indeed to be able to use the same side windows and only change the small cassettes when the test object will have to be lifted up. Another advantage was to keep the possibility to use several holes located on each side windows as pressure taps or probe access.

Another difficulty encountered in the design of this facility was to correctly seal the 2D sliding bump and prevent any leakage to the atmosphere. The first attempt consisted of minimising the small gap between the small cassette and the bump. This solution was abandoned due to scratches caused by the Plexiglas material on the soft Aluminium. The second attempt thus consisted of enlarging this gap

and use an inflated O-ring to seal the channel to the atmosphere. The idea was precisely to keep a small gap between the 2D bump and the Plexiglas to preserve both the bump surface and the hot film sensors. The measuring procedure will now consist of inflating the O-ring before the measurements, and deflate it before moving the 2D bump to the next position.

3D Bump

A second test object consists of a three-dimensional (3D) bump which was numerically designed to create varying mean flow gradients through the width of the test section. The design parameters were the varying length and thickness across the width of the bump, as well as the throat line position (Fig 9).

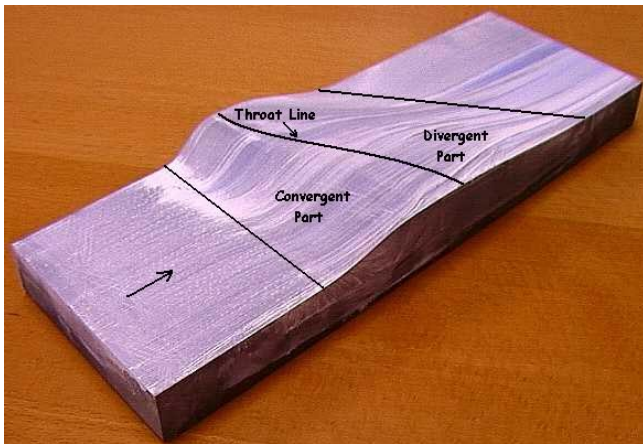


Figure 9: 3D bump

As a result of the special curvatures, a sonic pocket will develop itself on one side of the bump and a bent shock will occur over the throat line position. This special shape of the nozzle will allow to study the influence of the mean flow gradients on the shock motion.

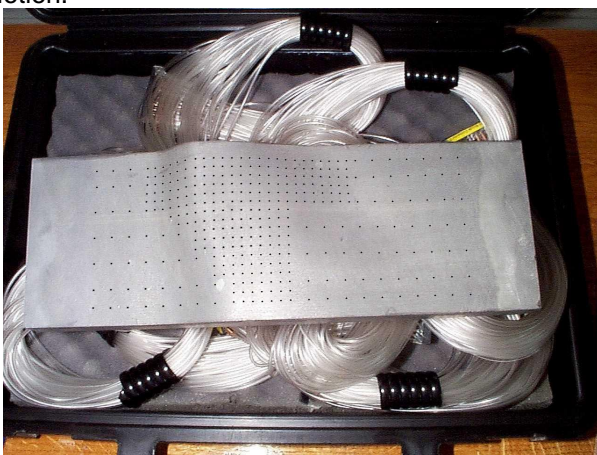


Figure 10: Instrumented 3D bump

Among four models available for instrumentation, one is already instrumented with 350 pressure taps (Fig.10). Here again, a special design of the pressure holes allows both steady and unsteady transducers to be inserted in any of the pressure taps covering the surface of the bump.

BACK PRESSURE FLUCTUATIONS GENERATOR

In order to study the unsteady shock motion and pressure distribution over the different test objects, a rotating ellipse placed downstream of the test section is used as a pressure wave generator. A high speed DC motor rotates this rod with a frequency up to 660 Hz. As the rod is alternatively aligned and perpendicular to the main flow direction, the losses created in the wake change periodically the outlet pressure. As a result, pressure perturbations propagate upstream at a speed which is function of the local flow velocity, and interact with the shock wave. An electronic control box features a feedback loop in order to maintain the rotation as constant as possible, and an optical encoder directly placed on the shaft is used to display the rotating speed with an accuracy of $\pm 0.5\%$.

PRESSURE HOLE CALIBRATION

With the aim to have a large amount of pressure taps on each test objects, the design was made standard to keep the possibility to exchange any transducer from one pressure hole to another. As a result, a small cavity does exist between the surface and the transducer, which has to be taken into account.

It has to be noted that the calibration procedure here addresses two primary issues: the determination of the relationship between the instrumentation output signal and the measured quantity, and the minimisation of the bias error. The latter, also called the systematic error, is inherent to the experiment and can be well determined and thereafter corrected by a good calibration.



Figure 11: Calibration Head (EPFL Calibration Unit)

The sensitivities of the unsteady pressure transducers will be determined using a device, which applies a periodic fluctuating pressure on the pressure tap. The design of this calibration unit (still being manufactured) was based on a device already existing and fully tested at EPFL. This apparatus consists of a small hand-held device (Fig.11) that is placed directly on the surface of the instrumented test object. This device contains a small chamber that is connected to an external source of pressure fluctuation (Fig.12). The interface between the tap surface and the chamber opening is sealed with an O-ring. The fluctuating pressure within the chamber is measured simultaneously by one reference transducer and the

transducer to be calibrated. Considering the size of the cavity within the small hand held device (Fig.11), it is assumed that the same pressure was immediately present at all transducers and the pressure tap on the surface. The different transducer voltages will be input into the K8000 system (described below) and a comparison of both the amplitude and phase shift will be made. The sensitivity of the given transducer is thereafter calculated based on this comparison and the known specifications (calibration curve) of the reference transducer.

The external source of pressure fluctuation of the apparatus consists of a cylinder with pockets on its circumference, which rotates in a casing with a relatively small gap at the circumference (Fig.12). The small pockets are alternately opened to a pressurised chamber and to the atmosphere. Openings situated in the casing, at the same height as the small pockets, are alternately exposed to the high and ambient pressure as the cylinder rotates. This fluctuating pressure is thereafter connected to the calibration head via a plastic tube, see Fig.11.

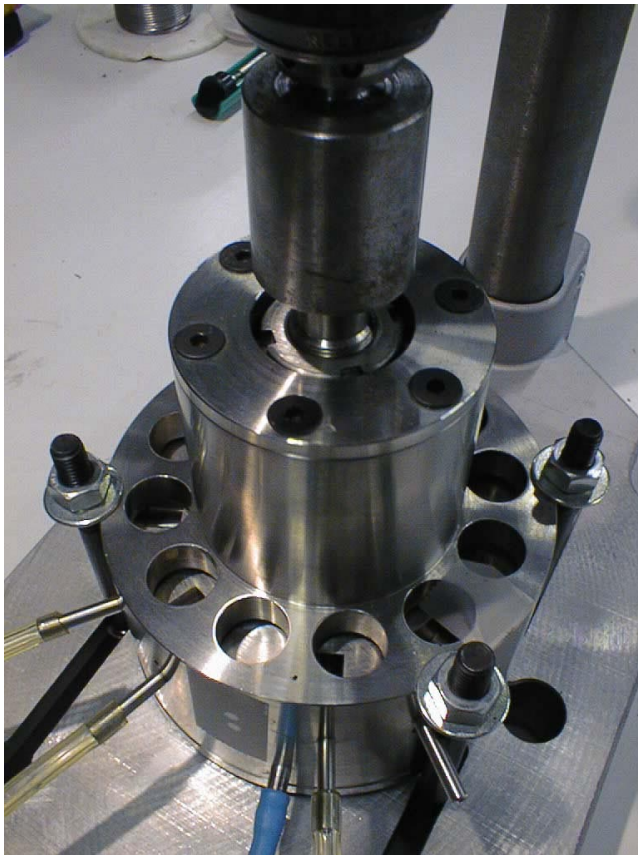


Figure 12: EPFL Calibration Unit

While the fluctuating pressure is close to a rectangular wave directly at the casing, higher frequencies are damped in the plastic tube. This however is not supposed to affect the calibration as the frequency components can be isolated by the signal analyser, and each frequency used for the calibration.

MEASURING TECHNIQUES

Steady state pressure measurements will be performed using a 208 channels data acquisition system (PSI 8400). Different Pressure Standard Units (PSU) are available and allow different pressure range measurements (7 kPa, 35 kPa, and 100 kPa relative to atmosphere) up to 300 Hz on each channel, with $\pm 0.05\%$ full scale accuracy.

Unsteady pressure measurements will be performed using a 32 channels data acquisition system from Kayser Threde (K8000). Each individual channel features a 100 kHz bandwidth differential input, programmable input voltage (5 mV to 5 V), programmable calibration and offset correction, a 12 Bit ADC with a maximum sampling rate of 1Msamples/s per channel, and a low pass filter 48 dB/Octave with programmable Cut Frequency. A sampling rate of 3.2 Msamples/s for all 32 channels (100 Ksamples/s per channel) and real time data storage is thus possible.

The boundary layer behaviour will be investigated with surface mounted hot films, hot wire traverses, LDA measurements and surface oil visualisations. A conventional Schlieren system is used to monitor the shock motion in the 2D nozzle using a high speed camera (up to 8000 pic/s). A state-of-the-art 3D-L2F will be employed to measure the 3D mean velocity vector and the turbulence intensity at the inlet boundary as well as at different stations in the test section. PIV measurements are also foreseen in the future.

PRELIMINARY RESULTS

In order to illustrate the preliminary results obtained in this new facility and thereby confirm the design objectives, the steady state pressure and oil surface visualisation on the 3D bump surface are presented below (figure 13 and 14).

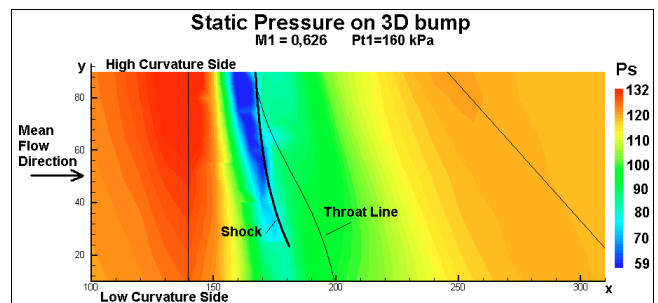


Figure 13: Steady State Pressure on 3D Bump Surface

It should first be noted that the dimension of the plot on Fig.13 does not represent the entire surface of the test object but the instrumented area only, which can be seen in Fig.10.

At the investigated operating point, a sonic pocket appears (in blue) on the "high curvature" side of the 3D bump, develops itself across the channel width, but does not reach the opposite side wall. As a result of

the inclined throat line, the shock wave is bent. The same observation can be made on figure 14, which clearly shows the streamlines in the BL as well as the separation bubble under the shock (in which some oil-paint mix stagnates).

A recirculation zone can also be seen in the corner just downstream of the bump, on the high curvature side. According to the streamlines, the flow in the BL seems to be highly deflected by this separation pocket.

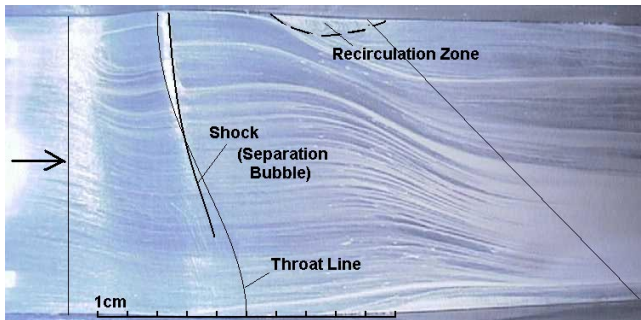


Figure 14: Oil Surface Visualisation on 3D Bump

Further steady and unsteady pressure measurements will be performed to investigate the unsteady interaction of upstream propagating pressure waves with a shock.

CONCLUSION

A project has been started at the Chair of Heat and Power Technology, Sweden, to investigate experimentally basic unsteady flow effects and interactions in internal transonic flows.

For this purpose, a highly modular facility has been specially redesigned and taken into service to study the unsteady interaction of upstream propagating pressure waves in transonic convergent-divergent nozzles. The facility also enables the investigation of unsteady flow transition in 2D nozzle and features a possible BL cut off. Moreover, different tests objects and several measuring techniques have been instrumented in this facility.

As the overall objective of the project is to get precise insight into aeroelastic phenomena and determine which parameter influences aeroelastic boundaries, further extended studies have already been planned. Among them, a flexible bump is to be implemented to simulate flow-structure interactions.

ACKNOWLEDGEMENT

The authors wish to thank STEM (project 6303) for their financial support.

REFERENCES

- [1] Atassi H.M.; Fang J.; Ferrand P.
"A study of the unsteady pressure of a cascade near transonic flow condition"
ASME paper 94-GT-476, June 1994
- [2] Atassi H.M.; Fang J.; Ferrand P.
"Acoustic blockage effect in unsteady transonic nozzle and cascade flows"
Symposium on Unsteady Aerodynamics and Aeroelasticity of Turbomachines, Tanida and Namba Editors, Elsevier, September 1994, pp. 777-794
- [3] David S.S.; Malcom G.N.
"Experiments in unsteady transonic flows"
AIAA/ASME/ASCE/AHS 20th Structure, Structural Dynamics and Material Conference
AIAA paper 79-769, pp. 417-433 St. Louis, M.O., 1979
- [4] Ekaterinaris J.; Platzer M.
"Progress in the Analysis of Blade Stall Flutter"
Symposium on Unsteady Aerodynamics and Aeroelasticity of Turbomachines, Tanida and Namba Editors, Elsevier, September 1994, pp. 287-302
- [5] Ferrand P.
"Etude theorique des ecoulements instationnaires en turbomachine axiale. Application au flottement de blocage."
State thesis, Ecole Centrale de Lyon, 1986
- [6] Ferrand P.; Atassi H.M.; Aubert S.
"Unsteady flow amplification produced by upstream or downstream disturbances"
AGARD, CP 571, January 1996, pp. 331.1-31.10
- [7] Ferrand P.; Atassi H.M.; Smati L.
"Analysis of the non-linear transonic blockage in unsteady transonic flows"
AIAA paper 97-1803, Snowmass, Col. USA, 1997
- [8] Ferrand P.; Aubert S.; Atassi H.M.
"Non-linear interaction of upstream propagating sound with transonic flows in a nozzle"
AIAA paper 98-2213, Toulouse, France, 1998
- [9] Gerolymos, G. A.; Bréus, J.-P.
"Computation of Unsteady Nozzle Flow due to Fluctuating Back-Pressure using Euler Equations."
ASME Paper No. 94-GT-91
- [10] Ott, P
"Oszillierender Senkrechter Verdichtungsstoß in einer Ebenen Düse."
Ph.D. Thesis at Ecole Polytechnique Federale de Lausanne; These No 985 (1991); 1992
- [11] Tijdman H.; Seebass R.
"Transonic flow past oscillating airfoils"
Annual Review of Fluid Mechanics, vol. 12, 1980, pp. 181-222
- [12] Klingmann, B. M.; 1997
private communication, 1997
- [13] Morel, Th.; 1977
"Design of Two-Dimensional Wind Tunnel Contractions."
Journal of Fluids Engineering, Vol. 99, pp. 371-378, 1977
- [14] Stratford, B. S.; 1959
"The Prediction of Separation of the Turbulent Boundary Layer."
Journal of Fluid Mechanics, Vol. 5, pp. 1-16, 1959